

Radiation of a uniformly moving line charge in a zero-index metamaterial and other periodic media

Avner Yanai and Uriel Levy*

Department of Applied Physics, The Benin School of Engineering and Computer Science, The Hebrew University of Jerusalem, Jerusalem, 91904, Israel

[*ulevy@cc.huji.ac.il](mailto:ulevy@cc.huji.ac.il)

Abstract: Radiation of electromagnetic waves by a uniformly moving charge is the subject of extensive research over the last several decades. Fascinating effects such as Vavilov-Cherenkov radiation, transition radiation and the Smith-Purcell effect were discovered and studied in depth. In this paper we study the radiation of a line charge moving with relativistic constant velocity within an average zero index metamaterial consisting of periodically alternating layers with negative and positive refractive index. We observe a strong radiation enhancement, ~ 3 orders of magnitude, for specific combinations of velocities and radiation frequencies. This surprising finding is attributed to a gigantic increase in the density of states at the positive/negative index boundary. Furthermore, we shed light on radiation effects of such a line charge propagating within the more “traditional” structure of periodically alternating layers consisting of positive and different refractive index with focus on frequencies satisfying the quarter wave stack and the half wave stack conditions. We show that the quarter-wave-stack case results in emission propagating vertically to the line charge trajectory, while the half-wave-stack results in negligible radiation. All these findings were obtained using a computationally efficient and conceptually intuitive computation method, based on eigenmode expansion of specific frequency components. For validation purposes this method was compared with the finite-difference-time-domain method.

© 2012 Optical Society of America

OCIS codes: (240.6690) Surface waves; (050.0050) Diffraction and gratings; (300.2140) Emission.

References and links

1. V. L. Ginzburg, “Radiation by uniformly moving sources (Vavilov - Cherenkov effect, transition radiation, and other phenomena),” *Usp. Fiz. Nauk* **166**, 1033–1042 (1996).
2. P. M. van den Berg, “Smith-Purcell radiation from a line charge moving parallel to a reflection grating,” *J. Opt. Soc. Am.* **63**, 689–698 (1973).
3. P. M. van den Berg, “Smith-Purcell radiation from a point charge moving parallel to a reflection grating,” *J. Opt. Soc. Am.* **63**, 1588–1597 (1973).
4. S. J. Smith and E. M. Purcell, “Visible light from localized surface charges moving across a grating,” *Phys. Rev.* **92**, 1069 (1953).
5. S. L. Chuang and J. A. Kong, “Enhancement of Smith-Purcell radiation from a grating with surface-plasmon excitation,” *J. Opt. Soc. Am. A* **1**, 672–676 (1984).
6. T. Ochiai and K. Ohtaka, “Electron energy loss and Smith-Purcell radiation in two- and three-dimensional photonic crystals,” *Opt. Express* **13**, 7683–7698 (2005).

7. L. Schächter, *Beam-Wave Interaction in Periodic and Quasi-Periodic Structures* (Springer, 1997).
8. I. A. Fainberg and N. A. Khizhniak, "Energy loss of a charged particle passing through a laminar dielectric," *Sov. Phys. JETP* **5** 720–729 (1957).
9. B. M. Bolotovskii, "Theory of Cherenkov radiation (III)," *Sov. Phys. Usp.* **4**, 781–811 (1962).
10. K. F. Casey and C. Yeh, "Transition radiation in a periodically stratified plasma," *Phys. Rev. A* **2**, 810–818 (1970).
11. L. Sh. Khachatryan, S. R. Arzumanyan, and W. Wagner, "Self-amplified Cherenkov radiation from a relativistic electron in a waveguide partially filled with a laminated material," *J. Phys.: Conf. Ser.* **357**, 012004 (2012).
12. G. Adamo, K. F. MacDonald, Y. H. Fu, C. M. Wang, D. P. Tsai, F. J. de Abajo, and N. I. Zheludev, "Light well: a tunable free-electron light source on a chip," *Phys. Rev. Lett.* **103**(11), 113901 (2009).
13. C. Luo, M. Ibanescu, S. G. Johnson, and J. D. Joannopoulos, "Cherenkov radiation in photonic crystals," *Science* **299**(5605), 368–371 (2003).
14. C. Kremers, D. N. Chigrin, and J. Kroha, "Theory of Cherenkov radiation in periodic dielectric media: emission spectrum," *Phys. Rev. A* **79**, 013829 (2009).
15. C. Kremers and D. N. Chigrin, "Spatial distribution of Cherenkov radiation in periodic dielectric media," *J. Opt. A* **11**, 114008 (2009).
16. V. G. Veselago, "The electrodynamics of substances with simultaneously negative values of ϵ and μ ," *Sov. Phys. Usp.* **10**, 509–514 (1968).
17. J. Lu, T. Grzegorzczuk, Y. Zhang, J. Pacheco Jr., B.-I. Wu, J. Kong, and M. Chen, "Cherenkov radiation in materials with negative permittivity and permeability," *Opt. Express* **11**, 723–734 (2003).
18. S. Xi, H. Chen, T. Jiang, L. Ran, J. Huangfu, B. I. Wu, J. A. Kong, and M. Chen, "Experimental verification of reversed Cherenkov Radiation in left-handed metamaterial," *Phys. Rev. Lett.* **103**, 194801 (2009).
19. S. N. Galyamin, A. V. Tyukhtin, A. Kanareykin, and P. Schoessow, "Reversed Cherenkov-Transition radiation by a charge crossing a left-handed medium boundary," *Phys. Rev. Lett.* **103**, 194802 (2009).
20. S. N. Galyamin and A. V. Tyukhtin, "Electromagnetic field of a moving charge in the presence of a left-handed medium," *Phys. Rev. B* **81**, 235134 (2010).
21. D. E. Fernandes, S. I. Maslovski, and M. G. Silveirinha, "Cherenkov emission in a nanowire material," *Phys. Rev. B* **85**, 155107 (2012).
22. V. V. Vorobev and A. V. Tyukhtin, "Nondivergent Cherenkov Radiation in a wire metamaterial," *Phys. Rev. Lett.* **108**, 184801 (2012).
23. Z. Mohammadi, C. P. Van Vlack, S. Hughes, J. Bornemann, and R. Gordon, "Vortex electron energy loss spectroscopy for near-field mapping of magnetic plasmons," *Opt. Express* **20**, 15024–15034 (2012).
24. M. G. Moharam, E. B. Grann, D. A. Pommet, and T. K. Gaylord, "Formulation for stable and efficient implementation of the rigorous coupled-wave analysis of binary gratings," *J. Opt. Soc. Am. A* **12**, 1068–1076 (1995).
25. L. Li, "Use of Fourier series in the analysis of discontinuous periodic structures," *J. Opt. Soc. Am. A* **13**, 1870–1876 (1996).
26. P. Lalanne and G. Morris, "Highly improved convergence of the coupled-wave method for TM polarization," *J. Opt. Soc. Am. A* **13**, 779–784 (1996).
27. A. F. Oskooi, D. Roundy, M. Ibanescu, P. Bermel, J. D. Joannopoulos, and S. G. Johnson, "MEEP: a flexible free-software package for electromagnetic simulations by the FDTD method," *Comput. Phys. Commun.* **181**(3), 687–702 (2010).
28. R. Petit, *Electromagnetic Theory of Gratings* (Topics in Applied Physics) (Springer, 1980).
29. A. Yanai, M. Orenstein, and U. Levy, "Giant resonance absorption in ultra-thin metamaterial periodic structures," *Opt. Express* **20**, 3693–3702 (2012).
30. J. D. Jackson, *Classical Electrodynamics*, 3rd ed. (Wiley, 1999).
31. J. D. Joannopoulos, S. G. Johnson, J. N. Winn, and R. D. Meade, *Photonic Crystals: Molding the Flow of Light*, 2nd ed. (Princeton University Press, 2008).
32. S. Nefedov and S. A. Tretyakov, "Photonic band gap structure containing metamaterial with negative permittivity and permeability," *Phys. Rev. E* **66**, 036611 (2002).
33. L. Wu, S. He, and L. F. Shen, "Band structure for a one-dimensional photonic crystal containing left-handed materials," *Phys. Rev. B* **67**, 235103 (2003).
34. S. Kocaman, M. S. Aras, P. Hsieh, J. F. McMillan, C. G. Biris, N. C. Panoiu, M. B. Yu, D. L. Kwong, A. Stein, and C. W. Wong, "Zero phase delay in negative-refractive-index photonic crystal superlattices," *Nat. Photon.* **5**, 499–505 (2011).
35. I. Shadrivov, A. Sukhorukov, and Y. Kivshar, "Complete band gaps in one-dimensional left-handed periodic structures," *Phys. Rev. Lett.* **95**, 193903 (2005).
36. F. J. García de Abajo and M. Kociak, "Probing the photonic local density of states with electron energy loss spectroscopy," *Phys. Rev. Lett.* **100**(10), 106804 (2008).
37. F. J. García de Abajo, "Optical excitations in electron microscopy," *Rev. Mod. Phys.* **82**, 209–275 (2010).

1. Introduction

Since the experimental manifestation of Vavilov and Cherenkov in 1934 and the following theoretical explanation by Frank and Tamm in 1937, it is known that a charged particle moving in a homogeneous medium with constant velocity larger than the phase velocity of light radiates electromagnetic energy. Other processes of radiation by charged particles with constant velocity are transition radiation and Smith-Purcell radiation [1–7]. Transition radiation occurs when the particle transverses materials with different refractive indexes. Smith-Purcell radiation is the consequence of converting the evanescent field (generated by a charged particle moving at a speed lower than the phase velocity of light in a medium) into propagating field by a diffraction grating. While the latter effect assumes the presence of a charged particle in vacuum, in close proximity to the grating, there is also a great interest in studying the radiation of charges moving at a constant velocity within the periodic media [8–12]. In [13] it was shown that line charges moving in a 2D photonic crystal may radiate in a reversed angle. In [14, 15] the radiation of both line charges and charged particles moving in photonic crystal lattices were analyzed.

In 1968, V. Veselago predicted that for a medium with negative ϵ and μ (a double negative (DNG) material) the Cherenkov radiation cone is reversed compared to the case of a medium with both ϵ and μ positive (a double positive (DPS) material) [16]. This prediction was later discussed in the context of lossy and dispersive DNG media [17] and confirmed experimentally [18]. The radiation of charged particles moving from DPS to DNG media was studied as well [19, 20]. Very recently, radiation in metamaterial wire grid media has been considered as well [21, 22]. Also has been considered the excitation of metamaterial structures with a magnetic dipole source [23].

In this paper, we combine the best of both worlds by addressing the problem of Cherenkov radiation resulted by a charged line source moving at a constant velocity within a periodic structure consisting of alternating DNG and DPS layers. We solve this problem using the Fourier modal method (FMM) [24–26], also known as the Rigorous Coupled Wave Analysis (RCWA) method. By this method, we find the eigenmode expansion of the radiation [6, 8, 14, 15]. In Section 2, we show how the radiation efficiencies are extracted using a FMM based algorithm that is both computationally efficient and conceptually simple. In Section 3, we validate the results using the Finite Difference Time Domain (FDTD) method [27], and calculate as an example the radiation pattern of a line charge moving within a quarter-wave stack (QWS) condition. It is shown that such a case results in vertical emission of electromagnetic wave. We also discuss the complimentary case of a half wave stack (HWS), producing negligible radiation. In Section 4, we show that when a line charge is moving within a DPS-DNG periodic structure a giant enhancement of the radiated field can be obtained, for specific combinations of frequencies and velocities.

2. Formulation of the problem

Our discussion begins with solving the electromagnetic fields in an infinite 1D periodic structure, excited by a line charge with infinite extent along the y direction which is moving at a relativistic velocity along the direction of periodicity (z). L is the unit cell size, v is the velocity of the line charge and ρ is charge density per unit length (see schematic in Fig. 1). The moving charge density results in a current density J in the z direction given by:

$$J_z(x, z, t) = \rho v \delta(x) \delta(z - vt) \quad (1)$$

where z is the direction of propagation. The periodic structure consists of two materials defined by their electric permittivity and magnetic permeability ϵ_i and μ_i ($i = 1, 2$) respectively, and by their width L_i . To calculate the electromagnetic fields that reside in this structure we first

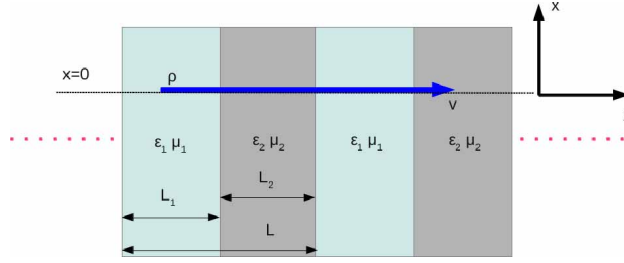


Fig. 1. Schematic drawing of the structure, extending infinitely in the x and y directions, with periodicity in the z direction. Two unit cells of the structure are shown. The thick blue arrow denotes the propagation direction of the line charge. $x = 0$ is defined as the x position of the line source.

calculate the eigenmodes of the structure for the homogeneous problem (in the absence of sources) using the FMM, and afterward extract the coupling of the source to the eigenmodes.

2.1. Homogeneous problem

We briefly review the essential basics of the FMM, while further details can be found in the references. In its most common formulation, the FMM uses a Floquet-Bloch expansion within a unit cell $0 \leq z < L$, to represent Maxwell's equations in an infinitely periodic structure. Afterwards, the eigenmodes and eigenvalues of the fields are calculated by solving an eigenvalue equation. We now elaborate on these principles. The Floquet-Bloch condition implies that the wavevectors in the z direction are given by $k_{z,m} = k_{z,0} + mK$, where $K = 2\pi/L$ is the grating vector and $k_{z,0}$ is the "zero-order" term, which is discussed in more detail in the next paragraph. The FMM allows to express the fields in the periodic structure as

$$F(x, z) = \sum_{m=-\infty}^{\infty} \sum_{n=1}^{\infty} W_{mn} C_n \exp(jk_{x,n}x) \exp(jk_{z,m}z) \quad (2)$$

Equation (2) can be simplified to: $F(x, z) = \sum_{m=-\infty}^{\infty} D_m(x) \exp(jk_{z,m}z)$ where $\underline{D} = \underline{W} \underline{X} \underline{C}$ is a column vector with elements corresponding to the Fourier components of the field, \underline{W} is a matrix with elements m, n (m being the Fourier order, and n being the eigenmodes index number [24]), \underline{X} is a diagonal matrix with elements $\exp(jk_{x,m}x)$, and \underline{C} is a column vector of coupling constants. Each diffracted order obeys the pseudo-periodic boundary conditions at the two unit cell boundaries $F(x, z=0) = F(x, z=L) \exp(jk_0L)$ [28]. For the described geometry, the line source excites only TM electromagnetic fields (single magnetic field component H_y and two electric field components E_x and E_z , and F describes one of these fields). Using the FMM approach, it is common to solve for the out-of-plane field component (H_y in our case), by solving numerically an eigenproblem for a truncated number of Fourier orders, resulting in finite sized matrices $(2N+1 \times 2N+1)$ and vectors $(2N+1 \times 1)$, where $2N+1$ is the number of Fourier orders used in the calculation. For the TM case, the equation needed to be solved is: $\frac{\partial^2}{\partial x'^2} H_y = (\underline{E} \underline{K}_z \underline{E}^{-1} \underline{K}_z - \underline{E} \underline{M}) H_y$ [24, 29] where x' is the normalized coordinate defined by $x' = k_0 x$ ($k_0 = 2\pi/\lambda_0$ with λ_0 being the vacuum wavelength of the electromagnetic wave), and \underline{E} , \underline{M} are the electric permittivity and magnetic permeability Toeplitz matrices respectively and \underline{K}_z is a diagonal matrix consists of the elements $(k_{z,0} + mK)/k_0$. By solving the eigenvalue problem, one obtains both the eigenvector matrix and eigenvalues $(k_x/k_0)^2$ of the emitted electromagnetic field. What remains to be found is the coupling constants vector \underline{C} , as discussed next.

2.2. Inhomogeneous problem

Our next step is to find the coupling of the current source to the various eigenmodes, which were calculated by solving the homogeneous eigenvalue problem. To accomplish this, we first transform the current source from time domain Eq. (1) to the frequency domain, yielding:

$$\tilde{J}_z(x, z, \omega) = \rho \delta(x) \exp(j \frac{\omega}{v} z) \quad (3)$$

Where the optical frequency $\omega = 2\pi c/\lambda_0$. The factor (ω/v) in the exponential argument in Eq. (3) may be interpreted as the spatial frequency of the current source [1], $k_{z,c} = \omega/v$. In an homogeneous medium, the current source will induce an electromagnetic wave with a spatial frequency $k_{z,c}$ along the z direction, similarly to the spatial frequency of the current source itself. Since $k_x^2 + k_{z,c}^2 = \epsilon\mu k_0^2$ it follows that for a homogeneous medium with a real and positive refractive index $n = \sqrt{\epsilon\mu}$, if $v < c/n$ then k_x is purely imaginary while for the case of $v > c/n$, k_x is real, resulting in a propagating wave. It is therefore convenient to rewrite Eq. (3) as:

$$\tilde{J}_z(x, z, \omega) = \rho \delta(x) \exp(jk_{z,c}z) \quad (4)$$

It is seen that the only non-zero Fourier spatial component of the source is $k_{z,c}$. We have already mentioned that by using Floquet-Bloch expansion the fields in the periodic structure can be described as asset of plane waves with wavevectors $k_{z,m} = k_{z,0} + mK$. One can therefore interpret the “zeroth order” ($m = 0$) wavevector of the diffraction problem $k_{z,0}$ to emanate from the spatial frequency of the source $k_{z,c}$. The periodic structure facilitates coupling to higher orders ($m \neq 0$). This description is in close analogy to the configuration of illuminating a periodic structure by a plane wave, where $k_{z,0}$ is the incident wavevector component along the direction of periodicity.

Equation (4) defines a surface current density, which forces a discontinuity of the magnetic field, equal to half the current amplitude [30]. Therefore, at an infinitesimal distance σ from $x = 0$, the magnetic field obeys:

$$2H_y|_{\sigma} = \rho \exp(jk_{z,c}z) \quad (5)$$

In order to find the coupling coefficients C , we combine Eqs. (2) and (5), obtaining:

$$\sum_{n=1}^{2N+1} C_n W_{mn} \exp(jk_{z,m}z) \exp(jk_{x,n}\sigma) = \frac{1}{2} \rho \exp(jk_{z,c}z) \quad (6)$$

Which can be written in matrix form as: $\underline{W} \underline{X} \underline{C} = \frac{1}{2} \rho \underline{\delta}_{m,0}$ where $\underline{\delta}_{m,0}$ is a column vector with all elements zero, except for the element corresponding to the zeroth order ($m = 0$) which is equal to unity. For $x \rightarrow 0$ the matrix \underline{X} is asymptotically equal to the identity matrix \underline{I} . The matrix \underline{W} is obtained by solving the homogeneous problem. It is now possible to solve for the column vector of coupling constants \underline{C} :

$$\underline{C} = \frac{1}{2} \rho \underline{W}^{-1} \underline{\delta}_{m,0} \quad (7)$$

Having obtained \underline{C} , we have a full description of H_y .

2.3. Calculation of radiated power

Using conservation of energy, the radiated electromagnetic power in the unit cell per frequency component is obtained by calculating the time averaged work done by the line charge.

$$P(\omega) = \frac{1}{2} \text{Re} \left(\iint_{\sigma,L} \tilde{J}_z E_z^* dx dz \right) \quad (8)$$

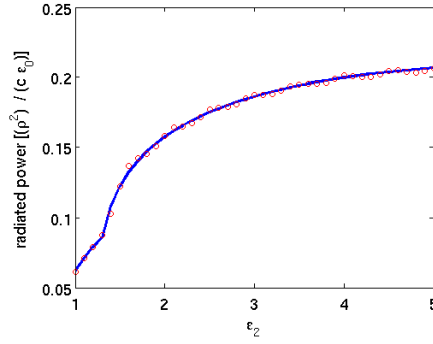


Fig. 2. Radiated power $P(\omega)$ from one unit cell, normalized by $\rho^2/(c\epsilon_0)$ as a function of ϵ_2 calculated for $\epsilon_1 = 1, \mu_1 = 1, \mu_2 = 2, v = 0.85c, L = 0.4536\lambda = 2L_1 = 2L_2$. The blue line and the red circles correspond to FMM and FDTD results respectively.

For TM polarization, the E_z field can be deduced from H_y . In matrix form we write [24]:

$$\underline{E}_z = \underline{E}^{-1} \underline{W} \underline{K}_x \underline{X} \underline{C} = \underline{V} \underline{X} \underline{C} \quad (9)$$

With \underline{V} defined as $\underline{V} = \underline{E}^{-1} \underline{W} \underline{K}_x$. Knowing E_z , Eq. (8) can be evaluated:

$$P(\omega) = \frac{1}{2} \text{Re} \iint_{\sigma, L} \rho \delta(x) \exp(jk_{z,c}z) \left(\sum_{m=-\infty}^{\infty} \sum_{n=1}^{\infty} V_{mn} C_n \exp(jk_{z,m}z) \right)^* dx dz \quad (10)$$

The delta function $\delta(x)$ removes the integration over x . By integrating over z , all multiplications between non equal Fourier components of the current source and E_z are zero from orthogonality, and Eq. (10) can be written in matrix form:

$$P(\omega) = \frac{1}{2} \rho L \text{Re}(\underline{V}_{m=0,n} \underline{C}) \quad (11)$$

where $\underline{V}_{m=0,n}$ is a row vector and its elements are the “zeroth order” Fourier components of each eigenmode.

We now show that the emitted power averaged over the unit cell is equal to the time averaged Poynting vector in the z direction $S_z = \frac{1}{2} \text{Re}(E_x H_y^*)$. Because of symmetry around $x = 0$, the time averaged Poynting vector is multiplied by two:

$$S_{z,tot} = \text{Re}(E_x H_y^*) = \text{Re} \left((\underline{V} \underline{C})(\underline{W} \underline{C})^T \right) = \frac{1}{2} \rho \text{Re} \left((\underline{V} \underline{C})(\underline{W} \underline{W}^{-1} \underline{\delta}_{m,0})^T \right) = \frac{1}{2} \rho \text{Re} \left((\underline{V}_{m=0,n} \underline{C}) \right) \quad (12)$$

In Eq. (12), “T” denotes the Hermitian complex conjugate transpose. It is seen that $S_z L = P$.

3. Simulation results

3.1. Comparison with FDTD

In order to validate our results, we now compare the total radiated power obtained with the FMM to FDTD simulations. In the FDTD model, we assumed a single wavelength current sheet source (infinite in the y direction and extending over the unit cell in the z direction) with angular frequency ω and $J_z(x, z, t) = \rho \delta(x) \exp(jk_{z,c}z) \exp(j\omega t)$. This current source represents

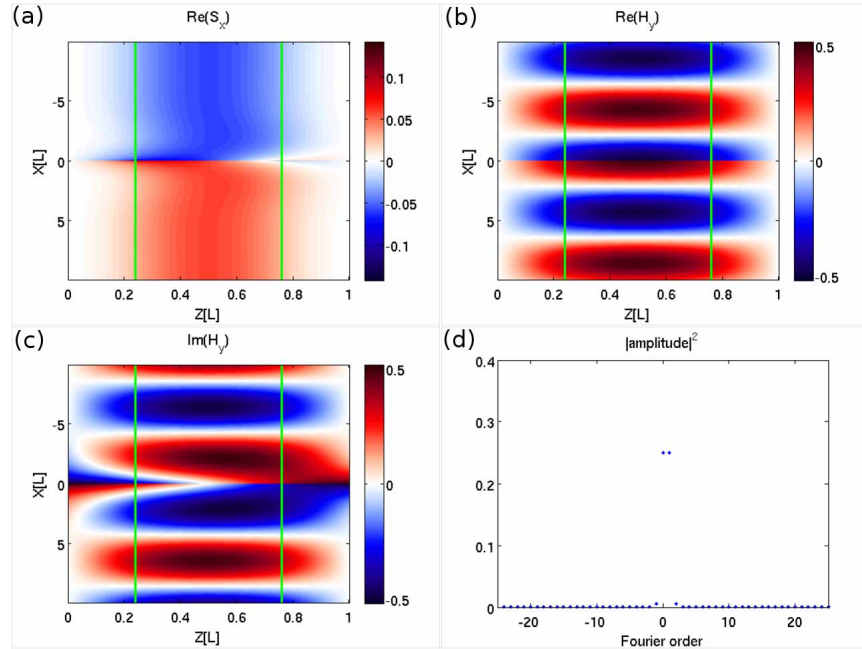


Fig. 3. (a) $\text{Re}(S_x)$ normalized by $\rho^2/(c\epsilon_0)$ (b,c) Field distribution of $\text{Re}(H_y)$ and $\text{Im}(H_y)$ (corresponding to an $\exp(j\omega t)$ time dependence) normalized by ρ . (d) Magnitude of the Fourier orders of H_y .

the steady state solution of our problem, i.e. it doesn't assume a moving line charge explicitly. As such, the current source excitation fits the purpose of validating the results obtained by FMM (being a frequency domain method the FMM provides a steady state solution) with an independent method. In Fig. 2 we show the radiated power per unit frequency as calculated by both FDTD and FMM. The consistency between the two methods is clearly evident.

3.2. Vertical emission from a periodic structure satisfying the QWS condition

We now consider the case of vertical emission of electromagnetic waves (light propagation along the x direction) by a line charge moving along the horizontal (z) direction within a 1D periodic structure. We focus our attention on a specific frequency (out of the continuum of frequencies emitted by the line charge) for which the QWS condition is satisfied. In a homogeneous medium, vertical emission is obtained when $k_{z,c}$ approaches zero. Unfortunately, such a case occurs only if the line charge is moving with an infinitely high velocity, and therefore vertical emission cannot be obtained in a homogenous medium. As known from the theory of 1D photonic crystals [31], Bloch wavevectors at one of the Brillouin Zone (BZ) edges (e.g. $k_B = \pi/L$, where k_B is the Bloch wavevector) with frequencies that obey the QWS condition, are Bragg reflected to the opposite Brillouin zone edge ($k_B = -\pi/L$). We now ask ourselves what would happen if we assume an excitation by a specific $k_{z,c}$ inducing a phase difference between the two boundaries of the QWS unit cell that is equivalent to $k_z = \pm\pi/L$, i.e. excitation at the edge of the 1st BZ. For such a case, all diffracted orders are located at the edges of this BZ. Obviously, these diffracted orders cannot contribute to power flow in the z direction, because all orders obey the QWS condition. Moreover, plane waves that monotonically decay in either the positive or negative z direction, cannot contribute to power flow in the x direction because their energy density vanishes. However, the superposition with equal phase and amplitude of

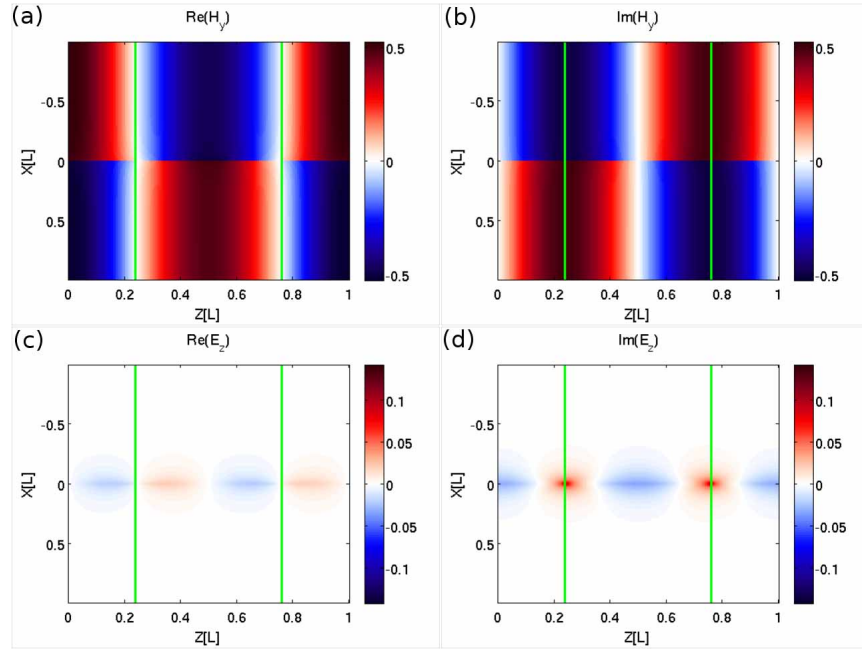


Fig. 4. (a,b) Field distribution of $\text{Re}(H_y)$ and $\text{Im}(H_y)$ (corresponding to an $\exp(j\omega t)$ time dependence), normalized by ρ . (c,d) Field distribution of $\text{Re}(E_z)$ and $\text{Im}(E_z)$ normalized by $\rho/(c\epsilon_0)$.

two such plane waves with their k_z at the opposite BZ edges, will result in a standing wave with zero phase difference across the unit cell, located at the center of the BZ ($k_z = 0$). Such a wave does not decay monotonically in the z direction and thus can propagate along the x direction.

Following this heuristic discussion we performed an FMM simulation with the following parameters obeying the QWS condition: $\lambda = 4L\sqrt{\epsilon_1\epsilon_2}/(\sqrt{\epsilon_1} + \sqrt{\epsilon_2})$, $v = 2Lc/\lambda$, $L_1 = \frac{\sqrt{\epsilon_2}}{\sqrt{\epsilon_1} + \sqrt{\epsilon_2}}L$, $L_2 = \frac{\sqrt{\epsilon_1}}{\sqrt{\epsilon_1} + \sqrt{\epsilon_2}}L$, $\epsilon_1 = 1.2$, $\epsilon_2 = 1$ and $\mu_1 = \mu_2 = 1$. In Fig. 3(a) the Poynting vector in the x direction (S_x) is shown, providing a clear evidence for the radiation of light in the vertical direction away from the line charge. In Figs. 3(b) and 3(c) we plot the real and imaginary parts of H_y (the colorbar is normalized by ρ). Indeed, one can learn from these two figures that away from the source (located at $x = 0$) the magnetic field has a negligible phase difference across the unit cell, as expected from the above mentioned discussion. In Fig. 3(d), we plot the magnitude of the Fourier components of the magnetic field amplitudes, (calculated at $x = \pm 100\lambda$ to diminish the effect of the non-propagating modes). As can be seen, there are two major non vanishing Fourier components ($N = 0, 1$), with equal amplitude. These two Fourier components correspond to plane waves with $k_z = \pm\pi/L$, in agreement with the above mentioned discussion. The phases of these two Fourier components (not shown) are identical. All Fourier orders are distributed symmetrically around $N = 0, 1$.

3.3. Horizontal emission from a periodic structure satisfying the HWS

We now study the emission from a HWS structure. We use similar parameters as in Section 3.2, only now $\lambda = 2L\sqrt{\epsilon_1\epsilon_2}/(\sqrt{\epsilon_1} + \sqrt{\epsilon_2})$ and $v = Lc/\lambda$. In Fig. 4 the field amplitudes of H_y and E_z are plotted. It is seen that in each half plane ($x > 0$ and $x < 0$), the magnetic field distribution corresponds to a “plane wave” propagating in the z direction. The E_z component decays expo-

nentially along the x direction and therefore S_x must be zero away from the source, as no power flux in the x direction can exist with a vanishing E_z component. Indeed, substituting our FMM results in Eq. (11) results in a null for the first nine significant digits behind the decimal point. The nearly zero radiated power is also understood from the following observation: the real and imaginary parts of the current distribution given by Eq. (4) are shifted by $\pi/2$ compared to the real and imaginary parts of E_z shown in Fig. 4. Therefore, the work done by the E_z field on the charges vanishes.

4. Radiation in zero real average refractive index DPS – DNG periodic structures

We now move forward to discuss the fascinating case of a current source moving within a HWS consisting of alternating DPS and DNG layers. In isotropic DPS media, the time averaged Poynting vector ($S = \frac{1}{2}\text{Re}(E \times H^*)$) and the wavevector k are parallel, while in isotropic DNG media they are anti-parallel [16]. Therefore, for the n th excited eigenmode with wavevector $k_{x,n}$, the Poynting vectors in the DPS and DNG media, are anti parallel. If the real part of the refractive index in the two media is opposite (as obtained for example for the following combination of parameters: $\varepsilon_1 = \varepsilon_R + j\varepsilon_I$, $\varepsilon_2 = -\varepsilon_R + j\varepsilon_I$, $\mu_1 = \mu_R + j\mu_I$, $\mu_2 = -\mu_R + j\mu_I$ where the subscripts R and I denote the real and imaginary parts of the material parameters respectively), and the duty cycle is set to $\frac{1}{2}$ (i.e. $L_1 = L_2$) the overall energy flow will cancel out after averaging over a unit cell, if the field intensities in both media are equal. This case of opposite real part of the refractive index is a special case of a structure having average zero real part of the refractive index [29, 32–34].

In Fig. 5(a), we plot the work done by the current source located within a DPS-DNG periodic structure as a function of v/c and λ/L , calculated for the following parameters: $\varepsilon_1 = 1 + 1 \times 10^{-3}j$, $\varepsilon_2 = -1 + 1 \times 10^{-3}j$, $\mu_1 = 1 + 1 \times 10^{-3}j$, $\mu_2 = -1 + 1 \times 10^{-3}j$ and $L = \lambda = 2L_1 = 2L_2$. Very narrow peaks are observed. Moreover, the calculated work reaches very high values: possibly three orders of magnitude higher than in “ordinary” DPS structures (compare with the values in Fig. 2). Figure 5(b) is based on similar data used in Fig. 5(a), however the v/c axis is now rescaled to $(\lambda/L) * (v/c)$. With this choice of scaling, the calculated work follows vertical lines located at $(\lambda/L) * (v/c) = \frac{1}{1}, \frac{1}{2}, \frac{1}{3}, \frac{1}{4}, \frac{1}{5}$ etc. (see also Fig. 5(c), where the color scale is saturated, making the locations more visible).

The drastically enhanced work stems from the fact that for $(\lambda/L) * (v/c) = 1/p$ (p is a natural number), $k_{z,c}L = 2\pi c/(\lambda v) = 2\pi p$. Comparing to Eq. (4), it follows that when $(\lambda/L) * (v/c)$ is equal to one of these discrete values, there is zero phase difference between the two boundaries of the unit cell. It was shown that for such a case, the local density of states (LDOS) is greatly enhanced [35]. Therefore, being proportional to the Cherenkov radiation [36,37], enhancing the LDOS must lead to the enhancement of the work done by the line charge. This effect cannot be observed in a standard DPS HWS because the field propagating along the z axis is not balanced by a counter propagating field, and thus there is no build up of the field. However, in the DPS-DNS case the propagation along the z axis in both media is opposite, giving rise to a resonance effect and high LDOS.

One must keep in mind that the enhancement factor depends on the losses within the material. For an ideal, nonrealistic case of zero loss one may expect an infinite enhancement, whereas for a higher loss scenario the enhancement will be diminished. Thus, this effect is expected to be observed primarily in the Giga Hertz to Tera Hertz frequency band, where the intrinsic loss of such materials is small.

Interestingly, while the product of JE^* is large due to the localized E_z field component, we did not observe coupling to radiative modes. This can be understood by the fact that the Poynting vector, averaged over the unit cell is identically zero due to the opposite power flow in both media.

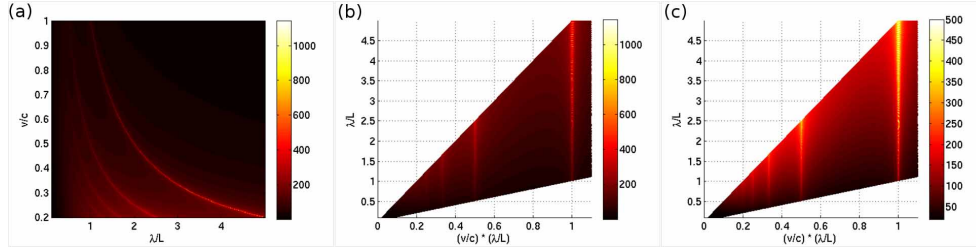


Fig. 5. (a) Work done by the line charge normalized by $\rho^2/(c\epsilon_0)$ as a function of λ/L and v/c . (b) Work done by the line charge normalized by $\rho^2/(c\epsilon_0)$ as a function of $(\lambda/L) * (v/c)$ and λ/L . (c) Same as (b) but with saturated color scale for visualization purposes.

The above mentioned discussion was based on an ideal, non dispersive case. While such an assumption is helpful in simplifying the understanding the very nature of light-matter interactions in the presence of constantly moving line charge, a full analysis must take dispersion into account. Evidently, in realistic dispersive media, obtaining a perfect matching of the refractive index in two adjacent layers over a broad frequency regime is challenging. We now consider the effect of dispersion by assuming a DNG medium to be dispersive: $\epsilon_2 = 1 - \omega_{p\epsilon}^2 / (\omega^2 + j\omega\gamma_\epsilon)$ and $\mu_2 = 1 - \omega_{p\mu}^2 / (\omega^2 + j\omega\gamma_\mu)$, with the following parameters: $\omega_{p\epsilon} = \sqrt{1.99}\pi c/L$, $\omega_{p\mu} = \sqrt{2.01}\pi c/L$, $\gamma_\epsilon = 1 \times 10^{-3}\omega_{p\epsilon}$ and $\gamma_\mu = 1 \times 10^{-2}\omega_{p\mu}$. For simplicity, the DPS medium is assumed to be air, i.e. $\epsilon_1 = 1$, $\mu_1 = 1$. For these assumed parameters, at $\lambda/L = 2$, the DNG constitutive parameters take the following values: $\epsilon_2 = -0.99 + 5.6 \times 10^{-3}j$ and $\mu_2 = -1.01 + 8.5 \times 10^{-3}j$. Comparing to the previous results, we find that the work is now lower by one order of magnitude (peak value is now $55 [\rho^2/(c\epsilon_0)]$) in the vicinity of $v/c = 0.5$ and $\lambda/L = 2$, where the FP condition is nearly satisfied). Additionally, the high work trajectory previously located at $(\lambda/L) * (v/c) = 1$ is no longer observed, because of the detuning from refractive index matching for wavelengths other than $\lambda/L = 2$.

5. Conclusions

Using the FMM, the radiation of line charges moving with relativistic constant velocity was studied. First, the FMM results were compared to FDTD. Subsequently, we showed that for frequencies satisfying the QWS condition, vertical emission is obtained, whereas the HWS case results in negligible emission. Following, we calculated the radiation of a line charge moving with relativistic constant velocity within an average zero index metamaterial consisting of periodically alternating layers with negative and positive refractive index. We observed a strong radiation enhancement, ~ 3 orders of magnitude, for specific combinations of velocities and radiation frequencies. The enhancement was attributed to the high local density of states at these frequencies. Finally, we considered the effect of dispersion. Evidently, significant enhancement is obtained even within dispersive media. Yet, the magnitude of enhancement is likely to be reduced in such practical scenario, owing to the difficulty in mitigating the challenge of perfect index matching, with the result of slight detuning from the FP condition.

Acknowledgments

The authors acknowledge the support of the Israeli Science Foundation (ISF). A.Y. acknowledges the support of the CAMBR and Brojde fellowships.